

Calorimetric study of calcium nitrate tetrahydrate and magnesium nitrate hexahydrate

Galina Sádovská¹ · Pavla Honcová¹ · Radim Pilař¹ · Lucie Oravová¹ · Daniel Honc²

Received: 2 August 2015 / Accepted: 12 November 2015 / Published online: 25 November 2015
© Akadémiai Kiadó, Budapest, Hungary 2015

Abstract The heat capacity and enthalpy of fusion of calcium nitrate tetrahydrate and magnesium nitrate hexahydrate were determined from 234.15 K to melting temperature by DSC. The modified stepwise method was used for heat capacity measurement, and enthalpy of fusion was determined from continuous heating by the rate of 10 K min⁻¹ (Pilař et al. in J Therm Anal Calorim 118:485–491, 2014). Determined values were used for the calculation of entropy and Gibbs energy in the experimental temperature range. Melting point and enthalpy of fusion of calcium nitrate tetrahydrate are 317.1 ± 0.3 K and 36.6 ± 0.2 kJ mol⁻¹, and for the magnesium nitrate hexahydrate, the values are 362.9 ± 0.4 K and 40.8 ± 0.5 kJ mol⁻¹. One solid–solid phase transformation was observed for the magnesium salt at 345.7 ± 0.9 K with enthalpy of transition 3.1 ± 0.2 kJ mol⁻¹. The available accumulated energy composed of sensible (heating) and latent heat (phase transformations) is 43.4 and 63.8 kJ mol⁻¹ for the hydrated calcium and magnesium nitrate, respectively. The kinetics of solid–solid phase transformation for magnesium salt was studied under non-isothermal conditions by DSC, and the process was described using autocatalytical

model with parameters in the range of 0.50–0.85 for m and range of 2.58–1.48 for n , respectively.

Keywords Calcium nitrate tetrahydrate · Magnesium nitrate hexahydrate · Heat capacity · Phase change materials · Kinetics · Autocatalytical model

Introduction

The compounds with a phase transformation covering melting of solid salt at suitable temperature can be used as phase change materials for thermal energy storage. Knowledge of their thermodynamic data is essential in the calculation of accumulated energy. Calcium nitrate tetrahydrate (Ca(NO₃)₂·4H₂O, CNT) and magnesium nitrate hexahydrate (Mg(NO₃)₂·6H₂O, MNH) can be used considering their melting point as low-temperature phase change materials (up to 200 °C) [2, 3].

The temperature of CNT melting is published in the range from 315.15 to 320.15 K with enthalpy of fusion having value from 28.7 to 36.1 kJ mol⁻¹ [2, 4–10]. Published values of heat capacity are often determined by one author for short temperature range [5, 8, 11, 12].

Magnesium nitrate hexahydrate shows solid–solid phase transition at around 345.15 K with enthalpy change of $\Delta_{\text{trs}} H = 3.1$ kJ mol⁻¹ [13, 14], and melts at about 363.15 K with enthalpy of fusion varied from 38.5 to 42.8 kJ mol⁻¹ [2, 4, 6, 7, 9, 13–17]. All data available in the literature are summarised with our results (described later).

This work focuses on the determination of heat capacity of Ca(NO₃)₂·4H₂O and Mg(NO₃)₂·6H₂O in broad temperature range (i.e. from 234.15 K up to the melting temperature of each substance). The temperature dependence of heat capacity is then used for the calculation of enthalpy,

Electronic supplementary material The online version of this article (doi:10.1007/s10973-015-5159-y) contains supplementary material, which is available to authorized users.

✉ Galina Sádovská
galina.sadovska@upce.cz

¹ Department of Inorganic Technology, Faculty of Chemical Technology, University of Pardubice, Doubravice 41, 53210 Pardubice, Czech Republic

² Department of Process Control, Faculty of Electrical Engineering and Informatics, University of Pardubice, Cs. Legii Sq. 565, 53002 Pardubice, Czech Republic

entropy and Gibbs energy changes as well as for the calculation of the amount of possible stored heat. The kinetics of solid–solid phase transformation for $\text{Mg}(\text{NO}_3)_2 \cdot 6\text{H}_2\text{O}$ was studied under non-isothermal conditions, and the suitable kinetic model was determined as well as the parameters of this model.

Experimental

Calcium nitrate tetrahydrate ($\text{Ca}(\text{NO}_3)_2 \cdot 4\text{H}_2\text{O}$, CNT) was of an analytical reagent grade (Penta, purity 99.0 %) as well as magnesium nitrate hexahydrate ($\text{Mg}(\text{NO}_3)_2 \cdot 6\text{H}_2\text{O}$, MNH) (Lachner, purity 99.0 %). Both chemicals were stored in a fridge. The exact amount of hydrate water was determined by chelatometric titration, and the average value was 3.98 and 6.07 mol for CNT and MNH, respectively. The structure of both substances was checked by X-ray diffraction analysis (Bruker AXE) performed at 298.15 K. Both chemicals were also characterised using thermogravimeter with differential thermal analyser DTA-TG (STA Jupiter 449, Netzsch). The apparatus has no cool accessory; therefore, the measurements start at the temperature of 303.15 K and finished at 423 K with the heating rate 5 K min^{-1} , sample mass about 200 mg and argon as protected atmosphere (flow $30 \text{ cm}^3 \text{ min}^{-1}$). DTA-TG measurements were taken mainly to verify the amount of water eliminated during dehydration.

The calorimetric measurements were taken using DSC Pyris 1 (Perkin-Elmer, USA) with Intracooler 2P. DSC was calibrated by the melting temperatures of pure metals (Hg, Ga, In, Sn, Pb and Zn), and the enthalpy change was calibrated using the fusion of indium. The samples (approximately 10 mg) were placed into the closed aluminium pans and measured in the atmosphere of dry nitrogen (flow $20 \text{ cm}^3 \text{ min}^{-1}$). The determination of accumulated heat energy includes the measurements of heat capacity and enthalpy of fusion or phase change, respectively. Heat capacity was determined from the measurements taken by the modified stepwise method [1]. This procedure requires not only baseline measurement but also one additional measurement with a standard reference material (sapphire, NIST standard reference material no. 720) using the same thermal program as in the case of studied sample. The optimal conditions of measurement in studied temperature range based on experiments with molybdenum as another standard material (NIST standard reference material no. 781D2) are described in paper [1] as well as uncertainty of calculated heat capacity of the sample which did not exceed 3 %. The “step” for heat capacity determination consists of 2 min of isotherm followed by heating step of 10 K by the rate of 5 K min^{-1} and finish by 1 min of isotherm. The heat capacity experiments were carried out

in the temperature range from 234.15 K to the melting temperature of each substance. The enthalpy of fusion was determined from heating by the rate of 10 K min^{-1} . The kinetics of phase change in MNH sample was studied in the temperature range of 223–423 K using several heating rates from 2 to 20 K min^{-1} .

Results and discussion

The diffraction patterns of the studied nitrates confirmed one phase composition corresponding diffraction lines in XRD database. The thermal behaviour of both studied samples was tested using thermogravimetric measurement from room temperature up to 423 K. In the case of calcium nitrate tetrahydrate, any sample mass change did not occur up to and during melting, but from 363 to 423 K, some water was evaporated (only 7.3 % of original sample mass). When the magnesium nitrate hexahydrate was heated, the mass started decreasing at the temperature of 353 K (i.e. during the phase change), but only 5.6 % of original sample mass left up to 423 K. These experiments have been done for the determination of water loss with significant higher amount of the samples than DSC experiment and with opened crucible. Therefore, the temperature of the phase transition is usually moved because of worse thermal conductivity of the larger sample. The gradual loss of structural water during (s)–(s) transition is eliminated by the use of closed pans in DSC experiments.

The isobaric heat capacity (C_p) was measured by modified stepwise method using DSC. This method is described in the literature [1] and is based on the comparison among baseline, standard material and sample DSC curves and the areas under these curves, respectively. The heat capacity of studied sample can be calculated using Eq. (1), where c_p is the isobaric specific heat capacity, m is a sample mass and A is the area under relevant curve. Subscript b stands for baseline, star in superscript is used for sapphire, and the values without star are for the sample.

$$c_p = c_p^* \left(\frac{m^*(A - A_b)}{m(A^* - A_b)} \right) \quad (1)$$

Values of the heat capacity of both salts were determined on DSC Pyris 1 in the temperature range from 234.15 K until melting point where each experimental point is calculated as the average of three independent measurements. Standard deviations are below 2 %, except for points near melting where the standard deviation was higher because of kinetics of melting. In the same temperature range, the polynomial functions were calculated according to

$$C_p (\text{J mol}^{-1} \text{K}^{-1}) = a + bT + cT^2 \quad (2)$$

with coefficient of determination $R^2 = 0.999$.

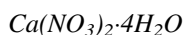
The change of enthalpy, entropy and Gibbs energy (ΔH , ΔS and ΔG) of tested solids were calculated from the temperature dependence of heat capacity according to Eqs. (3)–(5)

$$\Delta H = H_{T_2} - H_{T_1} = \int_{T_1}^{T_2} C_p(s) dT \tag{3}$$

$$\Delta S = S_{T_2} - S_{T_1} = \int_{T_1}^{T_2} \frac{C_p(s)}{T} dT \tag{4}$$

$$\Delta G = \Delta H - T\Delta S. \tag{5}$$

Heat capacity and thermodynamic properties



The experimental DSC and TG–DTA curves of continuous heating present one endothermic peak corresponding to melting of solid CNT. Enthalpy of fusion of CNT $\Delta_{fus}H = 36.6 \pm 0.2 \text{ kJ mol}^{-1}$ and melting point of CNT determined as the onset of the experimental DSC peak $T_m = 317.1 \pm 0.3 \text{ K}$ and the calculated entropy of fusion are comparable with published values in Table 1.

Progress of the temperature dependency of heat capacity of CNT is shown in Fig. 1, where is evident endotherm peak meaning melting of solid phase. Shorter temperature range (235–315 K) is inserted for better comparison of determined values with the literature data [11] with error bars $\pm 0.009 C_p$ [5] and $\pm 0.04 C_p$ [8].

Sufficiently high value of coefficient of determination of Eq. (2) in the temperature range is complying at upper temperature limit of 312.15 ($R^2 = 0.9997$). Final parameters of polynomial equation are given in Table 2. This temperature dependence of C_p was used for the calculation of enthalpy, entropy and Gibbs energy of CNT according to Eqs. (3)–(5), and result is summarised in Table 3 for the temperature range from 234.15 to 312.15 K.

Table 1 Melting point, enthalpy and entropy of fusion of CNT

T_m/K	$\Delta_{fus}H/kJ \text{ mol}^{-1}$	$\Delta_{fus}S/J \text{ mol}^{-1}K^{-1}$	References
315.65	31.1	98	[5]
320.15	33.6	105	[2]
315.85	29.7	94	[6]
315.85	32.2	102	[7]
316.05	34.1 ± 0.8	108	[8]
315.15	33.1	105	[4]
320.15	36.1	113	[9]
315.75	28.7	91	[10]
317.1 ± 0.3	36.6 ± 0.2	115 ± 1	This work

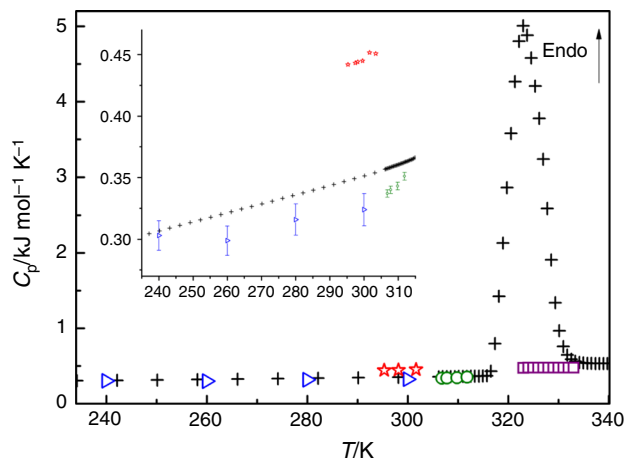


Fig. 1 Temperature dependence of the molar heat capacity of $Ca(NO_3)_2 \cdot 4H_2O$. Inset presents the temperature range of solid phase. Open green circle—[5], open blue right-pointing pointer—[8], open violet square—[11], open red star—[12], plus sign—this work. (Color figure online)

Table 2 Parameters (a , b , c) and correlation coefficient (R^2) of polynomial function (Eq. 2) of CNT fitted in the temperature range 234.15–312.15 K

Parameter	234.15–312.15 K
a	236 ± 5
b	-0.060 ± 0.037
c	$14.9 \times 10^{-4} \pm 0.7 \times 10^{-4}$
R^2	0.9997

Table 3 Enthalpy, entropy changes and Gibbs energy of CNT

T/K	$\Delta H/kJ \text{ mol}^{-1}$	$\Delta S/kJ \text{ mol}^{-1} K^{-1}$	$\Delta G/kJ \text{ mol}^{-1}$
234.15	0	0	–
239.15	1.53	0.38	–89.64
244.15	3.07	0.55	–130.30
249.15	4.63	0.64	–155.69
254.15	6.21	0.71	–174.98
259.15	7.80	0.77	–191.01
264.15	9.41	0.81	–205.04
269.15	11.04	0.85	–217.71
274.15	12.69	0.88	–229.42
279.15	14.36	0.91	–240.42
284.15	16.05	0.94	–250.87
289.15	17.75	0.96	–260.90
294.15	19.48	0.99	–270.58
299.15	21.23	1.01	–279.98
304.15	22.99	1.03	–289.16
309.15	24.78	1.04	–298.15
312.15	25.87	1.06	–303.47

Energy accumulation in material during heating can be described in terms of sensible and latent heat. The amount of stored sensible heat depends on the heat capacity of the material, and latent heat storage depends on the enthalpy change of phase transition. Combination of both gives amount of energy stored in the material which is heated from room temperature to melting and is described as

$$Q = \int_{298.15}^{T_m} C_p(s) dT + \Delta_{\text{fus}}H \quad (6)$$

with the result of the total accumulated energy for CNT of $Q = 43.4 \text{ kJ mol}^{-1}$.

$Mg(NO_3)_2 \cdot 6H_2O$

Calculated points of the temperature dependency of heat capacity of MNH are shown in Fig. 2 where two endothermic peaks are evident. First of them corresponds to (s)–(s) phase transition of $\alpha \rightarrow \beta$ and the second to melting of the solid phase. Pouillen [18] declared that at the temperature of 260.15 K, there is another endothermic effect of polymorphic transformation although Cantor [13] did not support this fact. However, comparison between wet and normal MNH sample showed (Fig. 3—insert) that effects below and around temperature of 273 K are caused by humidity condensed on MNH (sample taken from the fridge which is stored to prevent any change in the amount of hydrated water) and immediately measured, so that any phase change of MNH is not observed. The temperature of the only phase transition of MNH in our experimental temperature range was $T_{\text{trs}} = 345.7 \pm 0.9 \text{ K}$ with $\Delta_{\text{trs}}H = 3.1 \pm 0.2 \text{ kJ mol}^{-1}$, and the substance melts at the temperature $T_m = 362.9 \pm 0.4 \text{ K}$ with $\Delta_{\text{fus}}H =$

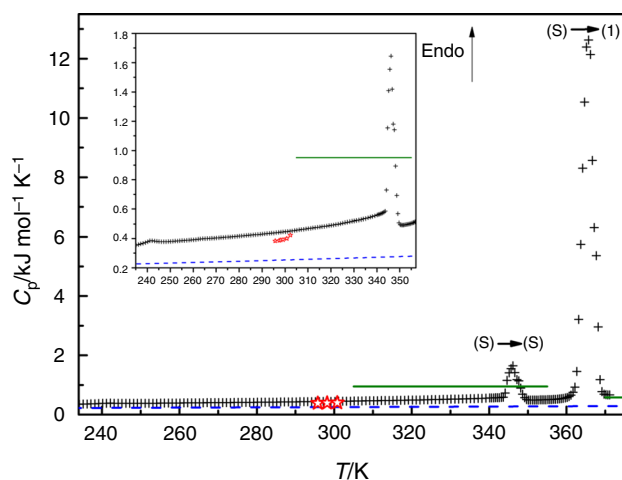


Fig. 2 Temperature dependence of the molar heat capacity of $Mg(NO_3)_2 \cdot 6H_2O$. Inset presents the temperature range of solid phase with (s)–(s) phase transition. Green solid line—[15], blue dashed line [27], open red star—[12], plus sign—this work. (Color figure online)

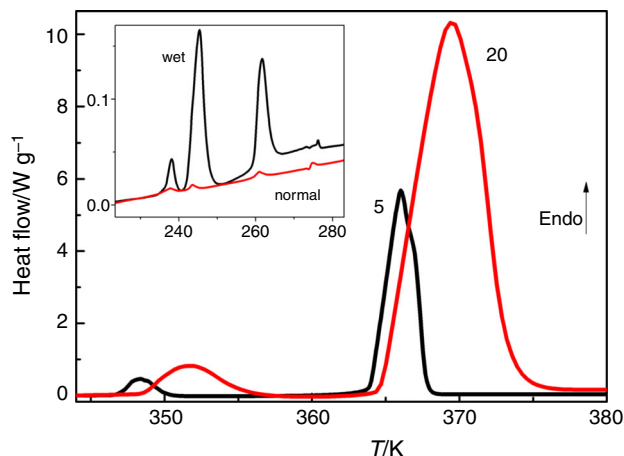


Fig. 3 Temperature dependence of heat flow for heating rate of 5 and 20 K min^{-1} . Inset figure shows heat flow dependence on temperature for wet and normal MNH sample heated by the rate of 10 K min^{-1}

$40.8 \pm 0.5 \text{ kJ mol}^{-1}$. All values are in good agreement with the literature data [2, 4, 6, 7, 9, 13–17] listed in Table 4.

The polynomial function expressing temperature dependency of heat capacity was determined for MNH in two temperature ranges divided by solid–solid transition from 234.15 K up to the temperature 343.65 K with the $R^2 = 0.99441$, and from 350.65 K and upper limit with $R^2 = 0.99875$, it was reached at the temperature 357.15 K. Therefore, the parameters of the polynomial function shown in Table 5 are fitted in two separate regions with break between 343.65 and 350.65 °C.

The temperature dependency of heat capacity was used for the calculation of the change of enthalpy, entropy and Gibbs energy (ΔH , ΔS and ΔG) of MNH according to Eqs. (3)–(5), and the obtained values are summarised in Table 6.

The total amount of accumulated energy of MNH was determined as sum of sensible heats, enthalpy of fusion and latent heat. MNH shows one phase transition from α to β modification and must be taken into account as is shown in Eq. (7).

$$Q = \int_{298.15}^{T_{\text{trs}}} C_p(s_\alpha) dT + \Delta_{\text{trs}}H + \int_{T_{\text{trs}}}^{T_m} C_p(s_\beta) dT + \Delta_{\text{fus}}H \quad (7)$$

The amount of stored energy when the MNH is heated from room temperature to melting is $Q = 63.8 \text{ kJ mol}^{-1}$.

Kinetics of solid–solid phase transformation of $Mg(NO_3)_2 \cdot 6H_2O$

The kinetics of modification change of MNH was studied using several heating rates from 2 to 20 K min^{-1} . Figure 3

Table 4 Temperatures and enthalpies of fusion and phase transition of MNH

T_{trs}/K	$\Delta_{\text{trs}}H/\text{kJ mol}^{-1}$	$T_{\text{m}}/^{\circ}\text{C}$	$\Delta_{\text{fus}}H/\text{kJ mol}^{-1}$	$\Delta_{\text{fus}}S/\text{J mol}^{-1} \text{K}^{-1}$	References
		363.15	41.0	113	[15]
		368.15	41.0	111	[2]
		362.45	38.5	106	[17]
346.15	3.1	363.15	38.9	106	[13]
		362.15	41.0	113	[4, 6]
344 ± 2	3.2	362.65 ± 0.5	38.5	106	[14]
		363.15	40.8	112	[7]
		362.2	41.7	115	[16]
		363.05	42.8	118	[9]
345.7 ± 0.9	3.1 ± 0.2	362.85 ± 0.4	40.8 ± 0.5	113	This work

Table 5 Parameters (a , b , c) and correlation coefficient (R^2) of polynomial functions (Eq. 2) of MNH

Parameter	234.15–343.65 K	350.65–357.15 K
a	1115 ± 38	56146 ± 2710
b	−6.50 ± 0.25	−318 ± 15.3
c	$11.4 \times 10^{-3} \pm 0.4 \times 10^{-3}$	0.455 ± 0.022
R^2	0.99441	0.99875

Table 6 Enthalpy, entropy changes and Gibbs energy of MNH

T/K	$\Delta H/\text{kJ mol}^{-1}$	$\Delta S/\text{kJ mol}^{-1} \text{K}^{-1}$	$\Delta G/\text{kJ mol}^{-1}$
234.15	0.00	0	–
239.15	1.85	1.40	−333.42
244.15	3.72	2.00	−484.55
249.15	5.60	2.35	−578.80
254.15	7.50	2.59	−650.29
259.15	9.43	2.77	−709.57
264.15	11.39	2.93	−761.31
269.15	13.37	3.05	−807.94
274.15	15.39	3.16	−850.91
279.15	17.44	3.25	−891.16
284.15	19.53	3.34	−929.31
289.15	21.66	3.41	−965.78
294.15	23.83	3.48	−1000.91
299.15	26.05	3.55	−1034.94
304.15	28.32	3.60	−1068.05
309.15	30.64	3.66	−1100.39
314.15	33.01	3.71	−1132.08
319.15	35.44	3.76	−1163.20
324.15	37.94	3.80	−1193.83
329.15	40.49	3.84	−1224.05
334.15	43.12	3.88	−1253.90
340.65	46.63	3.93	−1292.24

shows that the effect corresponding to the modification change is shifted to higher temperature with increasing heating rate, whereas the beginning of fusion (i.e. onset temperature) is almost independent on heating rate. The effect of modification change does not overlap with endothermic effect of fusion as is clearly seen in Fig. 3, and thus, standard kinetic analysis can be performed.

The measured heat flow Φ can be described by the kinetic equation [19]

$$\Phi = \Delta H A \exp\left(\frac{-E}{RT}\right) f(\alpha) \quad (8)$$

where ΔH is the enthalpy of the process (calculated from the area below the observed DSC peak, i.e. peak of solid–solid transformation), A is the pre-exponential factor, E is the apparent activation energy, R is a gas constant and T is temperature. The function $f(\alpha)$ is an analytical expression of the kinetic model where α is a degree of conversion. The data from DSC provide kinetic triplet necessary for further analysis: heat flow, temperature (or time in isothermal mode), conversion. Having these triplets, the kinetic analysis can be performed. During the kinetic analysis, first the apparent activation energy was calculated, then the applicability of commonly used models for description of modification change (such as nucleation-growth model, reaction order and autocatalytical model [19–21]) was tested, and finally, the parameters of the suitable model were calculated.

The most frequently used method of E evaluation—the Kissinger method [22], is applicable only for non-isothermal experiments where the temperature corresponding to the maximum of peak (T_p) shifts with the heating rate (β). The slope of the $\ln(\beta/T_p^2)$ dependence on $1/T_p$ is equal to the $-E/R$. Very similar is the Ozawa method [23] where the slope of the $\ln(\beta)$ dependence on $1/T_p$ is equal to $-1.052 E/R$. Both dependences of heating rate on $1/T_p$ are given in Fig. 4 from which is clearly seen that the value for 5 K min^{-1} is

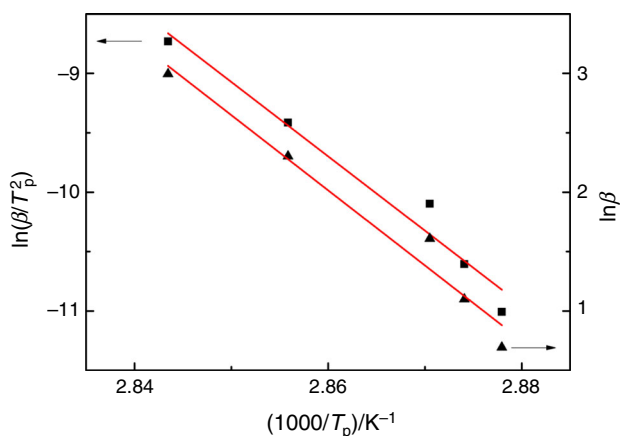


Fig. 4 Dependence of $\ln(\beta/T_p^2)$ and $\ln(\beta)$ on reciprocal value of temperature corresponding to the maximum of DSC peak

deviating from linear dependences. Thus, the activation energy determined by both methods has high error limits; E calculated by the Kissinger method is equal to $520 \pm 55 \text{ kJ mol}^{-1}$ and by Ozawa method $500 \pm 52 \text{ kJ mol}^{-1}$. Generally, Kissinger and Ozawa methods mainly differ only in one number (1.052), but using the Kissinger method is more frequented in the literature. However, there is only small difference between E value determined by Kissinger or Ozawa method and this difference is lower than error limits of E . It is only decision to further calculate with E determined by the Kissinger method.

The simplest way to test the applicability of commonly used model is the calculation of characteristic function $y(\alpha)$ and $z(\alpha)$ (Fig. 5) [20]. In non-isothermal conditions, the functions are defined as [21]:

$$y(\alpha) = \Phi \exp\left(-\frac{E}{RT}\right) \quad (9)$$

$$z(\alpha) = \Phi T^2 \quad (10)$$

In both cases, heat flow and temperature were taken from DSC results (corresponding to observed DSC peak, see Figs. 3, 6). These functions are normalised within the (0, 1) range (normalising means that minimum value of function equals to 0 and its maximum to 1), and they exhibit maxima at particular conversion which is signed as α_M for $y(\alpha)$ function and α_p^∞ for $z(\alpha)$ function, respectively. The exact values of these maxima or their relation as well as the shape of the curves $y(\alpha)$ and $z(\alpha)$ suggest a suitable kinetic model as is described in papers [21, 24]. As the $y(\alpha)$ and $z(\alpha)$ functions are invariable with respect to temperature or heating rate, being quite sensitive to subtle changes in the kinetic model $f(\alpha)$, they can be conveniently employed as suitable tools for the kinetic model determination [21].

Both functions were calculated from experimental data according to Eqs. (9)–(10). The illustration of the shape of

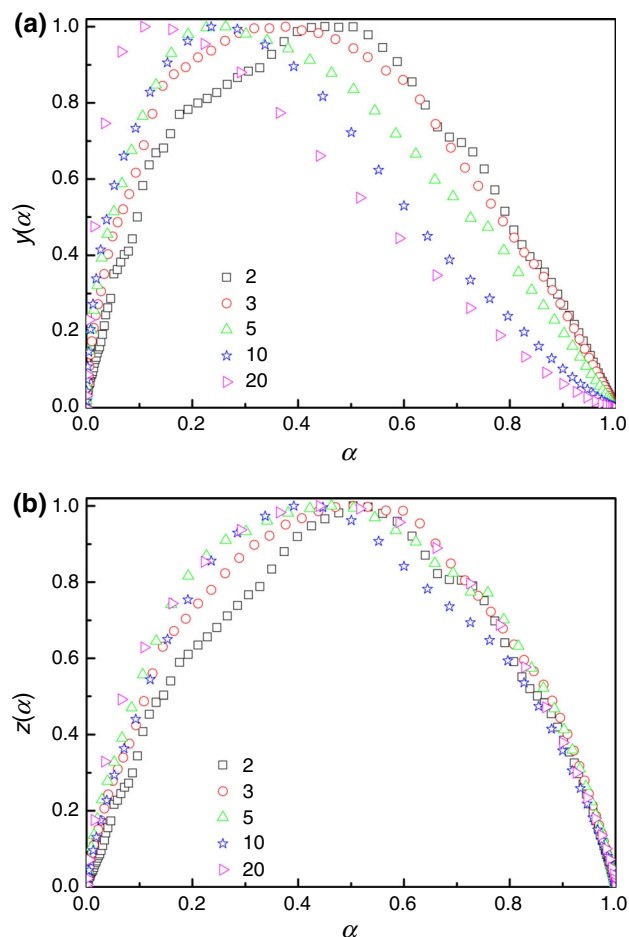


Fig. 5 Dependence of $y(\alpha)$ and $z(\alpha)$ function on conversion

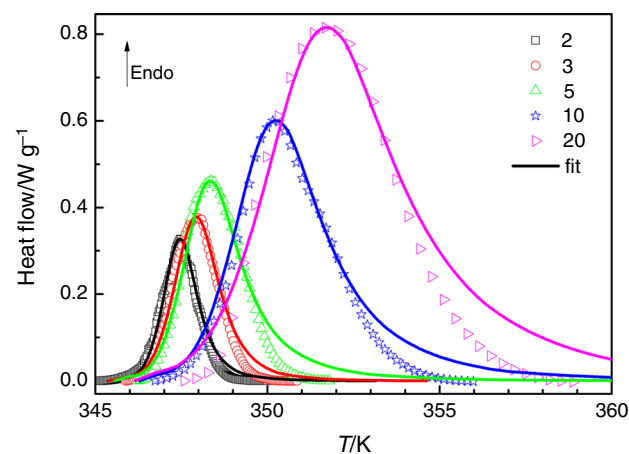


Fig. 6 Temperature dependence of heat flow for given heating rates. Points correspond to experimental data, and lines are calculated using parameters summarised in Table 7

these functions is shown in Fig. 5. Shape of $z(\alpha)$ function and conversion corresponding to the maximum of this function is not so different for all heating rates used. On the

Table 7 Parameters characterizing modification change effect for given heating rate: enthalpy change ΔH , conversion corresponding to the maximum of $y(\alpha)$ function α_M and $z(\alpha)$ function α_p^∞ , kinetic parameters calculated using E equal to 520 kJ mol⁻¹ are pre-exponential factor A , parameters of autocatalytical model m and n

Heating rate/K min ⁻¹	$\Delta H/J$ g ⁻¹	α_M	α_p^∞	$\ln(A/s^{-1})$	m	n
20	10.96	0.109	0.440	176.9	0.50	2.58
10	11.2	0.236	0.392	177.32	0.64	2.24
5	11.45	0.263	0.463	178.04	0.76	2.02
3	12.02	0.376	0.504	177.88	0.79	1.52
2	12.10	0.451	0.504	178.0	0.85	1.48

contrary, shape of $y(\alpha)$ function and conversion corresponding to the maximum of this function strongly depends on heating rate which means that the mechanism of observed process depends on heating rate.

The conversion corresponding to the maximum of characteristic functions (summarised in Table 7) fulfils the condition that $0 < \alpha_M < \alpha_p^\infty$ so only the autocatalytical model (AC) can be used to describe the observed process [24]. The autocatalytical model is an empirical model with parameters m and n [19]:

$$f(\alpha) = \alpha^m (1 - \alpha)^n \quad (11)$$

The autocatalytical model is an empirical model capable of describing kinetics of solid-state processes, although the parameters of this model have no physical meaning. However, from the mathematical point of view, they have to fulfil some conditions [25], e.g. $m < 1$.

The parameters of the model can be determined by the rearrangement of the experimental data [19, 20] or can be determined by the numerical fitting method [26]. The values of parameters of autocatalytical model and pre-exponential factor obtained by the numerical fitting are summarised in Table 7, and comparison of experimental data and calculated curves is given in Fig. 6. Similarly to $y(\alpha)$ function, the values of parameter m and n of AC model depend on heating rate used for DSC measurement. The value of parameter m is increasing from 0.50 to 0.85 with decreasing heating rate, whereas the value of parameter n is decreasing from 2.58 to 1.48. This significant change in parameters values should be a consequence of change in mechanism of observed process for different heating rates.

Conclusions

The precise measurement of the heat capacity of calcium nitrate tetrahydrate and magnesium nitrate hexahydrate was taken using DSC. Based on these results, other thermodynamic properties were calculated and amount of accumulated heat was calculated assuming heating of the substance from room temperature up to its melting

temperature. From the accumulated energy point of view, magnesium nitrate hexahydrate has higher accumulated ability caused by higher melting temperature as well as by the occurrence of two endothermic effects. However, the evaluation of ability of any substance for thermal energy storage can be done only when recovery of observed phase change is proved which needs additional analysis.

The phase transformation of magnesium nitrate hexahydrate was studied using different heating rates which enable kinetic analysis of obtained data. Results described in this paper showed that the process can be described by empirical autocatalytical model, where the values of its parameters depend on heating rate used. This means that the mechanism of observed process is changing with the heating rate.

References

- Pilař R, Honcová P, Košťál P, Sádovská G, Svoboda L. Modified stepwise method for determining heat capacity by DSC. *J Therm Anal Calorim.* 2014;118:485–91.
- Lorsch GH, Kauffman KW, Dentons JC. Thermal energy storage for solar heating and off-peak air conditioning. *Energy Convers.* 1975;15:1–8.
- Zalba B, Marín JM, Cabeza LF, Mehling H. Review on thermal energy storage with phase change: materials, heat transfer analysis and applications. *Appl Thermal Eng.* 2003;23:251–83.
- Voigt W, Zeng D. Solid-liquid equilibria in mixtures of molten salt hydrates for the design of heat storage materials. *Pure Appl Chem.* 2002;74:1909–20.
- Angell CA, Tucker JC. Heat capacities and fusion entropies of the tetrahydrates of calcium nitrate, cadmium nitrate, and magnesium acetate. Concordance of calorimetric and relaxational “ideal” glass transition temperatures. *J Phys Chem.* 1974;78:278–81.
- Guion J, Sauzade JD, Laügt M. Critical examination and experimental determination of melting enthalpies and entropies of salt hydrates. *Thermochim Acta.* 1983;67:167–79.
- Naumann R, Emons HH. Results of thermal analysis for investigation of salt hydrates as latent heat-storage materials. *J Thermal Anal.* 1989;35:1009–31.
- Xu Y, Hepler GL. Calorimetric investigations of crystalline, molten, and supercooled Ca(NO₃)₂·4H₂O and of concentrated Ca(NO₃)₂ (aq). *J Chem Thermodyn.* 1993;25:91–7.
- Sharma A, Tyagi VV, Chen CR, Buddhi D. Review on thermal energy storage with phase change materials. *Renew Sustain Energy Rev.* 2009;13:318–45.

10. Nikolova D, Maneva M. Thermal investigations of nitrate-hydrates and deuterates of Ca^{2+} , Cd^{2+} and Mg^{2+} . *J Therm Anal.* 1995;44:869–75.
11. Hattori T, Iwadata Y, Igarashi K, Kawamura K, Mochinaga J. Thermal characteristic of molten calcium nitrate tetrahydrate. *Denki Kagaku.* 1986;54:804–5.
12. Zhdanov VM, Shamova VA, Drakin SI. Heat capacity of crystal hydrates of magnesium, aluminum, calcium, nickel, and lanthanum nitrates and copper sulfate pentahydrate. Deposited Doc. VINITI. 1976;2874–76:1–10.
13. Cantor S. DSC study of melting and solidification of salt hydrates. *Thermochim Acta.* 1979;33:69–86.
14. Naumann R, Emons HH, Köhnke K, Paulik J, Paulik F. Investigation on thermal behaviour of $\text{Mg}(\text{NO}_3)_2 \cdot 6\text{H}_2\text{O}$. *J Therm Anal.* 1988;34:1327–33.
15. Riesenfeld EH, Milchsack C. Versuch einer Bestimmung des Hydratationsgrades von Salzen in konzentrierten Lösungen. *Zeitschrift für anorganische Chemie.* 1914;85:401–29.
16. Demirbas MF. Thermal energy storage and phase change materials: an overview. *Energy Source Part B.* 2006;1:85–95.
17. Nagano K, Ogawa K, Mochida T, Hayashi K, Ogoshi H. Thermal characteristics of magnesium nitrate hexahydrate and magnesium chloride hexahydrate mixture as a phase change material for effective utilization of urban waste heat. *Appl Therm Eng.* 2004;4:221–32.
18. Pouillen P. Les transformations polymorphiques des cristaux de nitrates de métaux bivalents hexahydratés. *CR Hebd Acad Sci.* 1960;250:3318–9.
19. Šesták J. Thermophysical properties of solids, their measurements and theoretical analysis. Amsterdam: Elsevier; 1984.
20. Málek J. Kinetic analysis of crystallization processes in amorphous materials. *Thermochim Acta.* 2000;355:239–53.
21. Málek J, Mitsuhashi T, Criado JM. Kinetic analysis of solid-state processes. *J Mater Res.* 2001;16:1862–71.
22. Kissinger HE. Reaction kinetics in differential thermal analysis. *Anal Chem.* 1957;29:1702–6.
23. Ozawa T. Kinetic analysis of derivative curves in thermal analysis. *J Therm Anal.* 1970;2:301–24.
24. Málek J. The kinetic-analysis of non-isothermal data. *Thermochim Acta.* 1992;200:257–69.
25. Málek J, Criado JM, Šesták J, Militký J. The boundary-conditions for kinetic-models. *Thermochim Acta.* 1989;153:429–32.
26. Málek J, Klikorka J. Crystallization kinetics of glassy GeS_2 . *J Therm Anal.* 1987;32:1883–93.
27. Yaws CL. Heat capacities of solids-elements and inorganic compounds. In: Yaws' handbook of thermodynamic properties for hydrocarbons and chemicals. Knovel. 2009. <http://app.knovel.com/hotlink/toc/id:kpYHTPHC09/yaws-handbook-thermodynamic/yaws-handbook-thermodynamic>. Accessed 31 March 2009.